ACS APPLIED MATERIALS & INTERFACES

Letter

www.acsami.org

# Tough and Biocompatible Hydrogels Based on in Situ Interpenetrating Networks of Dithiol-Connected Graphene Oxide and Poly(vinyl alcohol)

Gaolai Du, Lei Nie, Guorong Gao, Yuanna Sun, Ruixia Hou, Hua Zhang, Tao Chen, and Jun Fu*

Polymers and Composites Division, Ningbo Institute of Materials Technology & Engineering, Chinese Academy of Sciences, Zhongguan West Road 1219, Zhenhai District, Ningbo, Zhejiang 315201, P.R. China

Supporting Information

**ABSTRACT:** An interpenetrating network (IPN) strategy has been widely facilitated to construct strong and tough hydrogels, but most of the efforts have been focused on organic/organic networks. Herein, aqueous dispersible 2,2′-(ethylenedioxy)-diethanethiol (EDDET) cross-linked graphene oxide (E-cGO) skeleton was in situ incorporated into a PVA matrix, resulting in novel inorganic/organic IPN hydrogels with super mechanical and chondrocyte cell-adhesion properties. The unique interpenetrating structure and hydrogen bonding were demonstrated to play critical roles in enhancing the compressive property of the IPN hydrogels, in comparison to the GO and thermally reduced graphene oxide (T-rGO) filled hydrogels. It is critical that the E-cGO/PVA hydrogels have been demonstrated as being biocompatible, which make the E-cGO/PVA hydrogels promising candidate biomaterials for load-bearing biotissue substitution.

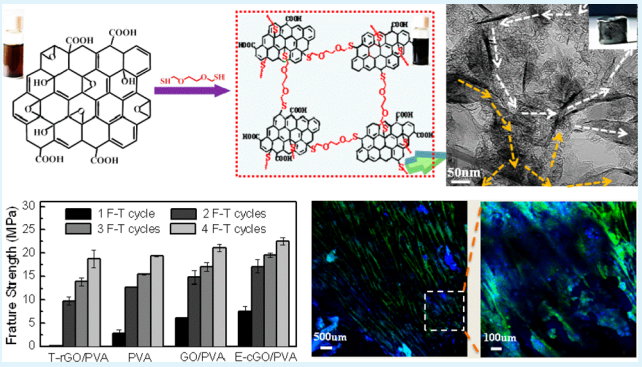


**KEYWORDS:** *inorganic/organic, IPN, tough, cell-adhesion, hydrogel*

Hydrogels with high strength, ductility, toughness, and low friction have been pursued for potential applications as load-bearing biotissue substitutes.[1−6] Multiple mechanisms have been combined with the concept of interpenetrating network (IPN) to create tough hydrogels with outstanding properties.[3,7] For example, double network (DN) hydrogels comprised of (semi-) interpenetrating polymer networks[3] have been widely reported to show tremendous enhancement of strength and toughness in comparison to the parent single network hydrogels. Current efforts have mostly been focused on organic−organic networks. The construction of inorganic/organic IPN structure that may combine the rigidity and strength of inorganic blocks with the flexibility of polymers has rarely been reported.

Graphene oxide (GO) or its derivatives possess high specific surface area, abundant functional groups, and extraordinary modulus and strength, and thus have been widely exploited to adsorb or cross-link polymer chains to produce tough and functional nanocomposite hydrogels.[8−12] Moreover, the ultra-high aspect ratio inspires the use of GO sheets as giant building blocks for the fabrication of nacre-like "mortar-brick" network structures.[13−16] Several "mortar" units including divalent cations ($Ca^{2+}$ and $Mg^{2+}$),[13] glutaraldehyde (GA) vapor,[14] 10,12-penta-cosadiyn-1-ol (PCDO),[15] or borate[16] have been used to fabricate biomimetic GO papers with excellent mechanical properties. Inspired by these studies, robust organic/inorganic IPN hydrogels consisting of interpenetrating GO and polymer networks have been developed. For example, GO network chelated by $Ca^{2+}$ ions has been utilized to intertwine with PAAm chains, generating highly stretchable IPN hydrogels.[12] The mechanical enhancements are usually limited by the inherent unstable feature of the physical association. Advances in fabrication of chemically bridged GO sheet networks with difunctional biomolecules are desired to create tough hydrogels with inorganic/organic IPN structures.

Herein, we report on a facile fabrication of tough and biocompatible hydrogels comprised of semi-IPN networks of biomolecule-cross-linked GO nanosheets and hydrophilic PVA chains. 2, 2′-(Ethylenedioxy)-diethanethiol (EDDET) is a small dithiol molecule and has been widely used as chain linker to create biocompatible monoliths.[17−19] Here, it is used to cross-link GO nanosheets through reactions between the thiol end groups with the functional groups on GO surface (Figure 1a). The EDDET-cross-linked graphene oxide (E-cGO) formed a stable homogeneous dispersion in water. On the other hand, GO nanosheets have a strong tendency to adsorb PVA chains, presumably driven by hydrogen bonding.[20] In this work, we proposed to perform one-pot simultaneous bridging of GO nanosheets with EDDET and in situ adsorption of PVA chains

**Received:** January 9, 2015
**Accepted:** January 26, 2015
**Published:** January 26, 2015





DOI: 10.1021/acsami.5b00184
*ACS Appl. Mater. Interfaces* 2015, 7, 3003−3008

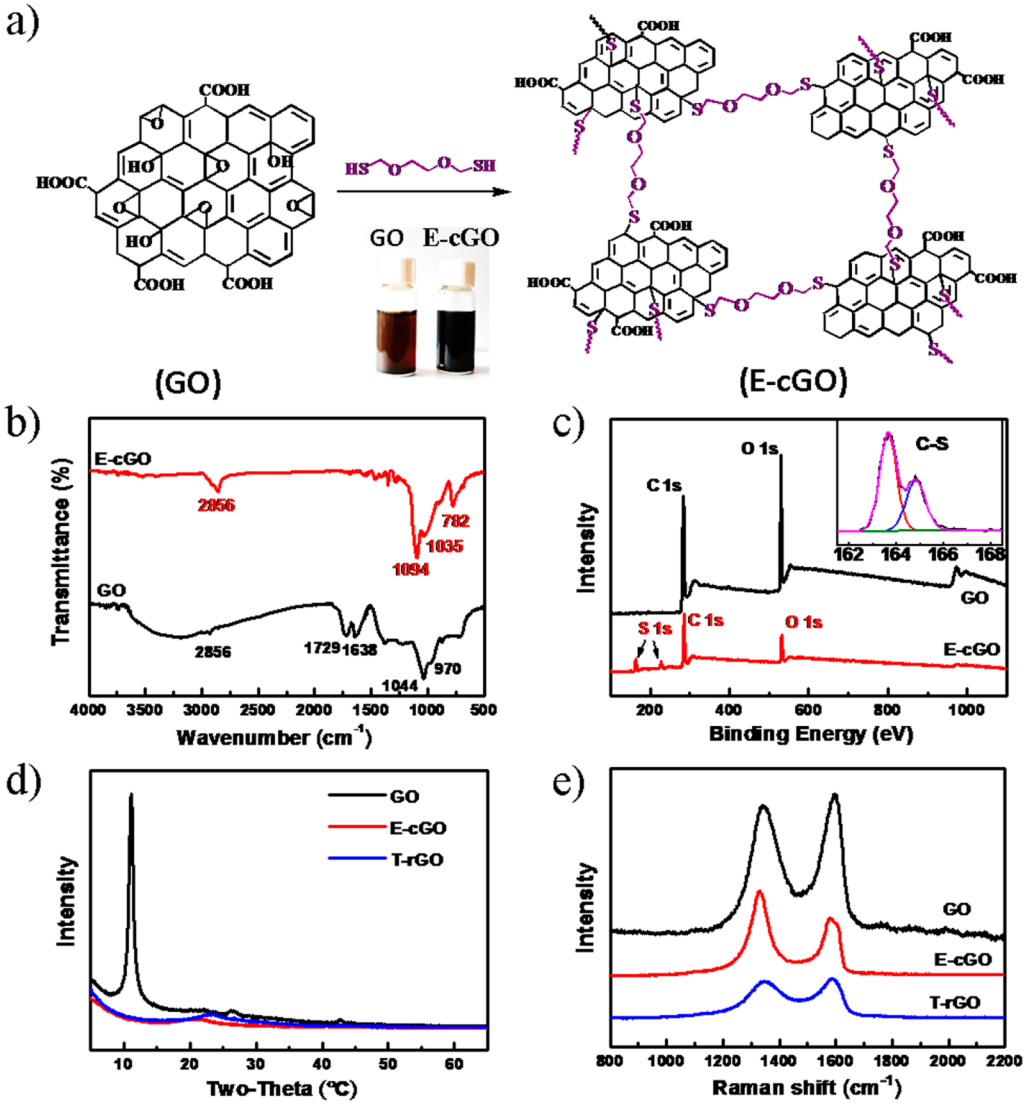


**Figure 1.** (a) Schematic illustration to the bridging of graphene oxide (GO) with EDDET molecules. The brownish GO dispersion was turned black after reaction with EDDET (inset). (b) ATR-IR and (c) XPS spectra of GO and EDDET-cross-linked GO (E-cGO). The inset shows the fitting of sulfur bands for E-cGO. (d) XRD and (e) Raman spectra of GO, E-cGO and thermally reduced GO (T-rGO) powders.

to the cross-linked GO blocks, with a purpose to create inorganic/organic IPN hydrogels for potential applications as load-bearing biotissue substitutes.

The reaction of EDDET with graphene oxide was successfully demonstrated and resulted in stable dispersion in water. Graphite oxide was synthesized by using a modified Hummers' method[21,22] and exfoliated to form brownish graphene oxide dispersion in water (Figure 1a). Atomic force microscopy revealed a graphene oxide monolayer with an average thickness of 0.91−1.2 nm (Figure S1, Supporting Information in the Supporting Information). To the brownish GO dispersion (100 mL), EDDET (2.58 mM) was added under continuous magnetic stirring at 90 °C, resulting in a homogeneous black dispersion in 30 min (Figure 1a). The dispersion was stable for months with a GO concentration up to 3 mg/mL. These results suggest the effective modification of GO with the dithiol molecules, which even provided excellent stability to the resulted aqueous dispersion.

The chemical modification of graphene oxide with EDDET (Figure 1a) was examined by using attenuated total reflection-infrared (ATR-IR) spectroscopy and X-ray photoelectron spectroscopy (XPS). The IR band at 3200 $cm^{-1}$ of GO surfaces was dramatically depressed after reaction with EDDET (Figure 1b). The epoxy C−O bands of GO at 1044 and 970 $cm^{-1}$ were significantly weakened for the EDDET-modified GO pellet. These results, together with the C−S band[23] at 782 $cm^{-1}$ and C−O bands at 1094 and 1035 $cm^{-1}$ from EDDET, confirmed the reaction between thiol groups and functional groups on GO surface (see Scheme S1 in the Supporting Information). XPS data of modified GO pellet further showed the presence of C−S bonds, which is absent for GO (Figure 1c). These results demonstrate the successful bonding of EDDET molecules on the GO surface.

The EDDET-cross-linked GO (E-cGO) powders were investigated by X-ray diffraction (XRD) and Raman spectroscopy. Pristine GO and thermally reduced GO (T-rGO)[24] were used as controls. The XRD pattern of E-cGO (Figure 1c) exhibited a wide and weak diffraction centered at $2\theta$ = 20.92°, indicating a reduced layer distance $d$ = 0.42 nm between the E-cGO sheets, in comparison to GO ($d$ = 0.75 nm). This is a little larger than that of T-rGO ($2\theta$ = 22.83°, $d$ = 0.39 nm), which could be attributed to both cleavage and bonding effect by


DOI: 10.1021/acsami.5b00184
ACS Appl. Mater. Interfaces 2015, 7, 3003−3008

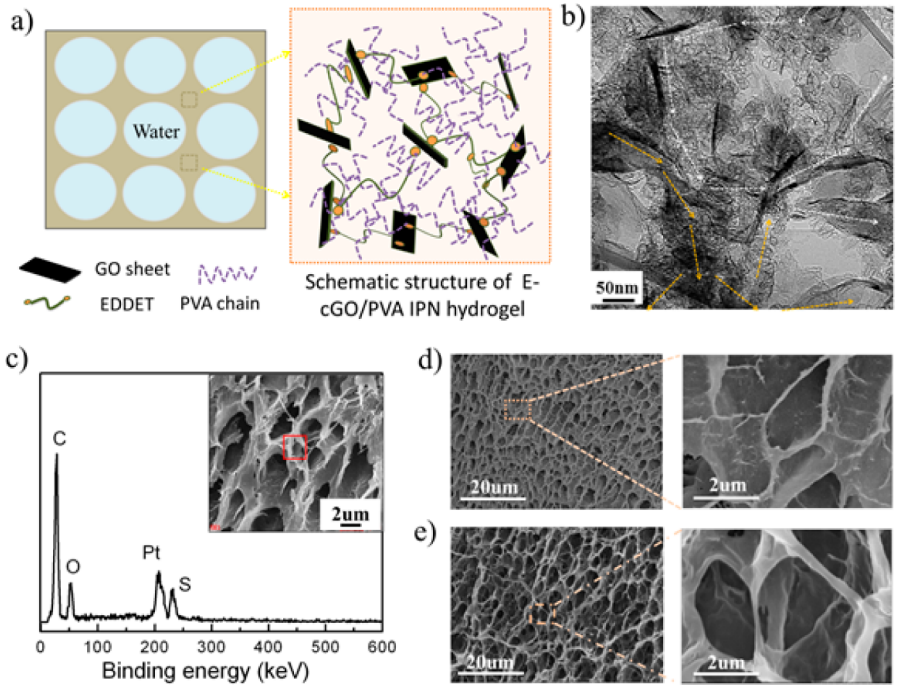


**Figure 2.** (a) Schematic illustration to the E-cGO/PVA IPN hydrogel. (b) Representative TEM image of the E-cGO$_{1.0}$/PVA-2 hydrogel. (c) EDS spectrum of the E-cGO$_{1.0}$/PVA-2 hydrogel. SEM images of (d) PVA-2 and (e) E-cGO$_{0.5}$/PVA-2 hydrogels.

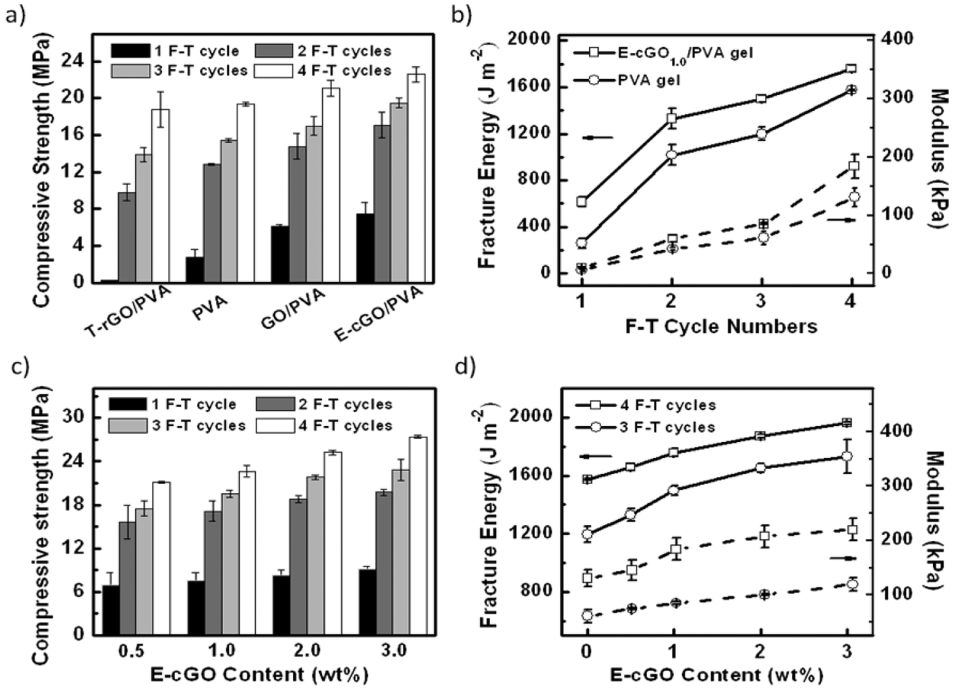


**Figure 3.** (a) Compressive strength of T-rGO$_{1.0}$/PVA, PVA, GO$_{1.0}$/PVA, and E-cGO$_{1.0}$/PVA hydrogels. (b) Fracture energy and modulus of PVA and GO$_{1.0}$/PVA with one to four F-T cycles. (c) Compressive stress of IPN hydrogels with E-cGO content. (d) Fracture energy and modulus of IPN gels with E-cGO content from the 3rd F-T cycle.

EDDET. Raman spectra of all the samples exhibited typical D band and G band (Figure 1e), with the intensity ratio ($I_D/I_G$) increasing from 0.92 (GO) to 0.97 (T-rGO) and 1.11 (E-cGO). These results indicate the increasing breakage of the GO carbon planar because of the thermal and chemical treatments.[25]

On the basis of the results shown above, we further demonstrated a one-pot synthesis of E-cGO in the aqueous PVA solutions, leading to in situ adsorption and penetrating of PVA chains into the E-cGO network. Specifically, EDDET (2.58 mM) and PVA (10 g) were dissolved in 100 mL of GO dispersion (1−3 mg/mL) under stirring at 90 °C for 2 h, resulting in homogeneous black suspension stable for months. The dispersion experienced freeze−thawing (F-T) to create E-cGO$_x$/PVA-$y$ IPN hydrogels,[26] where $x$ and $y$ represent the E-


DOI: 10.1021/acsami.5b00184
ACS Appl. Mater. Interfaces 2015, 7, 3003−3008

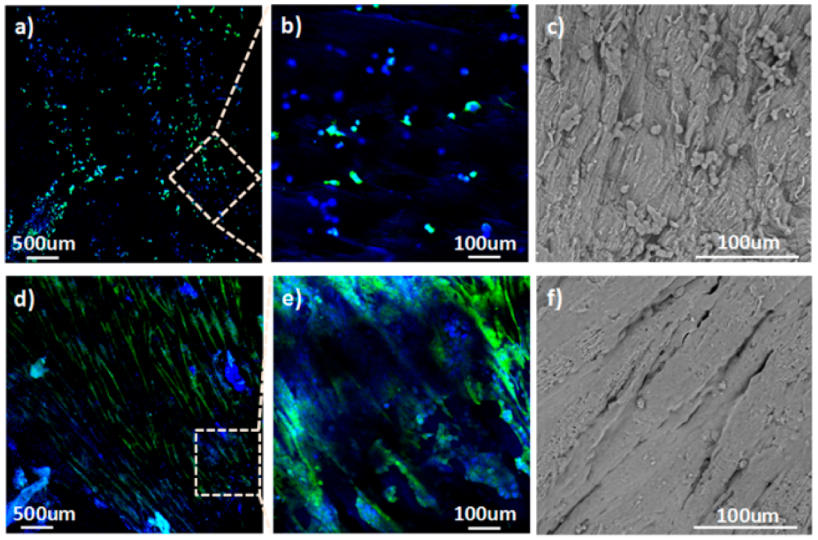


**Figure 4.** Fluorescent images of human chondrocytes seeded and cultured on (a, b) PVA-2 and (d, e) E-cGO$_{3.0}$/PVA-2 hydrogels for 6 days. SEM images of human chondrocytes cultured on (c) PVA-2 and (f) E-cGO$_{3.0}$/PVA-2 hydrogels for 6 days.

cGO content (weight percentage to PVA) and the F-T cycle number, respectively.

TEM images provide a direct evidence to the stacked and connected GO nanosheets in the PVA matrix (Figure 2b).The lateral dimensions of these E-cGO nanosheets were smaller than the pristine GO, presumably due to the chemical breakage of the planar during reaction with EDDET (Figure 1e). Energy-dispersive spectroscopy (EDS) analysis was utilized to investigate the element compositions in PVA, E-cGO and E-cGO/PVA samples. The E-cGO powders showed a sulfur content of 10.5 ± 2.6 at %, which confirmed the presence of EDDET (see Figure S2 in the Supporting Information). Correspondingly, the E-cGO/PVA hydrogel showed a 2.1 ± 0.1 at% sulfur content (Figure 2c), which is attributed to the presence of EDDET-modified graphene oxide in the PVA hydrogel.

The introduction of E-cGO showed a significant influence on the wall of the pores in the hydrogels (see Figure S3 in the Supporting Information). The presence of E-cGO resulted in a dramatic increase in the wall thickness of the dehydrated gels (about 200 nm) in comparison to that of neat PVA gels (about 45 nm) (Figure 2d, e). The wall originated from the phase separation of PVA crystallites and ice during freezing.[26,27] With the increase in E-cGO, the equilibrium water content of the E-cGO/PVA-2 hydrogels was decreased from 90.3 ± 0.1% to 88.5 ± 0.2%, which is higher than that of PVA-2 (88.2 ± 0.1%). To investigate the effect of E-cGO on the crystallization of PVA, we conducted wide-angle X-ray diffraction (WAXD) on PVA and E-cGO/PVA aerogels. The E-cGO/PVA samples showed lower diffraction intensities, suggesting a lower crystallinity of the IPN hydrogels than PVA (see Figure S4a in the Supporting Information). The presence of E-cGO network may impede the PVA crystallization.[24,28] In the freeze−thawed hydrogels, the relatively low crystallinity of E-cGO/PVA gels may suggest a lower cross-link density. This was verified by the larger equilibrium ratio of the E-cGO/PVA hydrogels (2.95 ± 0.15) than that of PVA hydrogels (1.79 ± 0.19) under swelling (see Figure S4b in the Supporting Information).

The E-cGO/PVA IPN hydrogels showed enhanced mechanical properties in comparison to neat PVA hydrogels. Figure S5 in the Supporting Information exhibits representative compressive stress−strain curves of PVA and E-cGO$_{1.0}$/PVA experiencing two F-T cycles. The E-cGO$_{1.0}$/PVA-2 showed a compressive modulus (the slope of stress−strain curves at 10−20% strain) of 60.0 ± 5.6 kPa and a fracture strength of 17.1 ± 1.4 MPa, in contrast to 42.3 ± 2.7 kPa and 12.8 ± 0.1 MPa for PVA. Another important property is the fracture toughness, which is defined as the area underneath the force−displacement curves to measure the capability to dissipate energy during loading.[2] The E-cGO$_{1.0}$/PVA-2 hydrogels showed a fracture toughness of 1328.4 ± 90.3 J m$^{-2}$, in contrast to 1016 ± 88.9 J m$^{-2}$ for the PVA-2 hydrogel. Moreover, with increasing F-T cycles, the modulus, fracture strength, and toughness of the E-cGO$_{1.0}$/PVA IPN hydrogels were further enhanced (Figure 3a, b).

We demonstrated that the unique interpenetrating structure and hydrogen bonding play critical roles in enhancing the compressive property of the nanocomposite hydrogels. The compressive properties of IPN hydrogels were compared with PVA hydrogels filled with 1 wt % GO and T-rGO. Interestingly, for hydrogels experiencing up to four F-T cycles, the E-cGO$_{1.0}$/PVA and GO/PVA hydrogels showed higher modulus and compressive strength than T-rGO/PVA gels (Figure 3b). In the former hydrogels, PVA chains may actively adsorb onto the GO and E-cGO sheets via hydrogen bonding.[19] In contrast, this may be difficult for T-rGO sheets as most of their functional groups are cleaved upon thermal treatments. Moreover, it is likely that the T-rGO nanosheets may aggregate and phase separate from the hydrophilic PVA matrix during F-T process. This explains the results that the IPN and GO-filled PVA hydrogels showed higher strength and modulus than neat PVA gels, while the T-rGO-filled PVA hydrogels appeared the weakest. It is of particular interest to investigate the strength and toughness of the IPN and GO-filled hydrogels with the same nanosheet content. The strength of IPN hydrogels was always higher than the GO-filled hydrogels with up to four F-T cycles (Figure 3b). This result further confirms the strengthening effects of the E-cGO network and IPN structures in contrast to unmodified GO nanosheets.

The mechanical properties of the E-cGO/PVA hydrogels were enhanced with the increasing E-cGO content for different F-T cycles. The compressive strength of E-cGO$_{0.5-3}$/PVA-3


DOI: 10.1021/acsami.5b00184
ACS Appl. Mater. Interfaces 2015, 7, 3003−3008

gels was increased from 17.5 ± 1.0, 19.5 ± 0.5, to 21.8 ± 0.3, and 22.8 ± 1.5 MPa (Figure 3c). Interestingly, the fracture energy and modulus of IPN hydrogels showed a monotonically increase with increasing E-cGO content for 3 F-T cycles (Figure 3d). The E-cGO$_{0.5}$/PVA-3 hydrogel exhibited a fracture energy of 1331.0 ± 41.9 J m$^{-2}$. As the E-cGO content was increased to 3 wt %, the compressive toughness of the hydrogel was further improved to 1731.3 ± 114.8 J m$^{-2}$. It is noted that the fracture toughness values of these E-cGO/PVA hydrogels are higher than that of articular cartilage (~1000 J m$^{-2}$). Mechanically, these E-cGO/PVA IPN hydrogels may be promising for applications as artificial cartilages.

Finally, we assessed the biocompatibility of these hydrogels by cell seeding and in vitro culture experiments. E-cGO/PVA-2 hydrogel discs (diameter = 9 mm, thickness = 2 mm) with 1−3 wt % E-cGO were seeded with human chondrocytes (Passage 4, 1.4 × 10$^5$ cells/mL) and cultured for 1, 3, and 6 days. At the specific culture time, the hydrogels were taken out from the media, blocked with glutaraldehyde, and stained with DAPI and/or FITC-phalloidin for imaging by using a confocal laser scanning microscope (CLSM). Herein, DAPI stained the E-cGO/PVA IPN substrates while FITC-phalloidin did not (see Figure S6 in the Supporting Information). Qualitative assessment of cell adhesion and growth on the IPN hydrogels is primarily based on the green fluorescence from FITC-phalloidin that preferentially stained to the cytoskeleton (see Figure S7 in the Supporting Information).[29] As a control, only a few cells were found on PVA hydrogels after 6 day's culture (Figure 4a−c), which is due to the intrinsic cell nonadhesive nature of PVA hydrogels. On the other hand, GO based material has been demonstrated to favor cell adhesion and proliferation.[30] CLSM images of hydrogels stained by FITC-phalloidin showed that the E-cGO/PVA-2 hydrogels nicely support the adhesion and proliferation of chondrocytes, in sharp contrast to PVA. The cell number density was increased over time (see Figure S7 in the Supporting Information). SEM images further revealed the nicely spread conformation of the chondrocytes on the hydrophilic surface of the E-cGO/PVA hydrogels (see Figure S8 in the Supporting Information). The cells excreted extracellular molecules and formed a thin layer on top of the E-cGO/PVA hydrogel substrate (Figure 4d−f). Moreover, the apparent cell number density seemed increased with increasing E-cGO content. These results suggest that the E-cGO/PVA hydrogels are favorable to cell adhesion and proliferation, which is probably due to the presence of GO and EDDET.

In conclusion, strong and tough hydrogels have been fabricated by using a one-pot method to synthesize EDDET-cross-linked GO network with the presence of PVA chains. It has been demonstrated by spectroscopy that the difunctional EDDET molecules reacted with and likely bridged the GO nanosheets into E-cGO networks. Meanwhile, the residual functional groups on the EDDET-modified GO may allow for the formation of hydrogen bonding with PVA chains, presumably resulting in a semi-interpenetrating network. Subsequent cyclic freeze−thawing led to nanocomposite hydrogels with improved strength and toughness, in comparison to pure PVA hydrogels. It is critical that both GO and EDDET, as well as the E-cGO/PVA hydrogels, have been demonstrated biocompatible. Thus, the nanocomposite hydrogels showed excellent biocompatibility and nicely supported chondrocyte adhesion and growth. We conclude that the E-cGO/PVA hydrogels may be promising candidate biomaterials for load-bearing biotissue substitution.

## ■ ASSOCIATED CONTENT

### Supporting Information

Experimental section and additional figures and data. This material is available free of charge via the Internet at http://pubs.acs.org/.

## ■ AUTHOR INFORMATION

### Corresponding Author

*E-mail: fujun@nimte.ac.cn.

### Notes

The authors declare no competing financial interest.

## ■ ACKNOWLEDGMENTS

This work was funded by the Hundred Talents Program of the Chinese Academy of Sciences (J.F.), and the Zhejiang Natural Science Foundation of China (LR13B040001).

## ■ REFERENCES

(1) Shin, M. K.; Spinks, G. M.; Shin, S. R.; Kim, S. I.; Kim, S. J. Nanocomposite Hydrogel with High Toughness for Bioactuators. *Adv. Mater.* **2009**, *21*, 1712−1715.

(2) Sun, J.-Y.; Zhao, X.; Illeperuma, W. R. K.; Chaudhuri, O.; Oh, K. H.; Mooney, D. J.; Vlassak, J. J.; Suo, Z. Highly Stretchable and Tough Hydrogels. *Nature* **2012**, *489*, 133−136.

(3) Gong, J. P. Why are Double Network Hydrogels so Tough? *Soft Matter* **2010**, *6*, 2583−2590.

(4) Han, Y.; Bai, T.; Liu, W. Controlled Heterogeneous Stem Cell Differentiation on a Shape Memory Hydrogel Surface. *Sci. Rep.* **2014**, *4*, 5815.

(5) Kamata, H.; Akagi, Y.; Kayasuga-Kariya, Y.; Chung, U.-i.; Sakai, T. "Nonswellable" Hydrogel Without Mechanical Hysteresis. *Science* **2014**, *343*, 873−875.

(6) Zhang, Y. Y.; Li, Y. M.; Liu, W. G. Dipole−Dipole and H-Bonding Interactions Significantly Enhance the Multifaceted Mechanical Properties of Thermoresponsive Shape Memory Hydrogels. *Adv.Funct. Mater.* **2015**, *25*, 471−480.

(7) Zhao, X. Multi-scale Multi-mechanism Design of Tough Hydrogels: Building Dissipation into Stretchy Networks. *Soft Matter* **2014**, *10*, 672−687.

(8) Liu, J. Q.; Chen, C. F.; He, C. C.; Zhao, L.; Yang, X. J.; Wang, H. L. Synthesis of Graphene Peroxide and Its Application in Fabricating Super Extensible and Highly Resilient Nanocomposite Hydrogels. *ACS Nano* **2012**, *6*, 8194−8202.

(9) Liu, R.; Liang, S.; Tang, X. Z.; Yan, D.; Li, X.; Yu, Z. Z. Tough and Highly Stretchable Graphene Oxide/polyacrylamide Nanocomposite Hydrogels. *J. Mater. Chem.* **2012**, *22*, 14160−14167.

(10) Lu, J. Y.; He, Y. S.; Cheng, C.; Wang, Y.; Qiu, L.; Li, D.; Zou, D. R. Self-Supporting Graphene Hydrogel Film as an Experimental Platform to Evaluate the Potential of Graphene for Bone Regeneration. *Adv. Funct. Mater.* **2013**, *23*, 3494−3502.

(11) Cha, C.; Shin, S. R.; Gao, X.; Annabi, N.; Dokmeci, M. R.; Tang, X.; Khademhosseini, A. Controlling Mechanical Properties of Cell-laden Hydrogels by Covalent Incorporation of Graphene Oxide. *Small* **2014**, *10*, 514−523.

(12) Cong, H.-P.; Wang, P.; Yu, S. H. Highly Elastic and Superstretchable Graphene Oxide/Polyacrylamide Hydrogels. *Small* **2014**, *10*, 448−453.

(13) Park, S.; Lee, K. S.; Bozoklu, G.; Cai, W.; Nguyen, S. T.; Ruoff, R. S. Graphene Oxide Papers Modified by Divalent Ions-Enhancing Mechanical Properties via Chemical Cross-linking. *ACS Nano* **2008**, *2*, 572−578.

(14) Gao, Y.; Liu, L. Q.; Zu, S. Z.; Peng, K.; Zhou, D.; Han, B. H.; Zhang, Z. The Effect of Inter layer Adhesion on the Mechanical



DOI: 10.1021/acsami.5b00184
*ACS Appl. Mater. Interfaces* 2015, 7, 3003−3008

Behaviors of Macroscopic Graphene Oxide Papers. *ACS Nano* **2011**, *5*, 2134−2141.
(15) Cheng, Q.; Wu, M.; Li, M.; Jiang, L.; Tang, Z. Ultratough Artificial Nacre Based on Conjugated Cross-linked Graphene Oxide. *Angew. Chem., Int. Ed.* **2013**, *52*, 3750−3755.
(16) An, Z.; Compton, O. C.; Putz, K. W.; Brinson, L. C.; Nguyen, S. T. Bio-lnspired Borate Cross-Linking in Ultra-Stiff Graphene Oxide Thin Films. *Adv. Mater.* **2011**, *23*, 3842−3846.
(17) Rydholm, A. E.; Bowman, C. N.; Anseth, K. S. Degradable Thiol-acrylate Photopolymers: Polymerization and Degradation Behavior of an in situ Forming Biomaterial. *Biomaterials* **2005**, *26*, 4495−4506.
(18) Kwisnek, L.; Goetz, J.; Meyers, K. P.; Heinz, S. R.; Wiggins, J. S.; Nazarenko, S. PEG Containing Thiol-Ene Network Membranes for $CO_2$ Separation: Effect of Cross-Linking on Thermal, Mechanical, and Gas Transport Properties. *Macromolecules* **2014**, *47*, 3243−3253.
(19) Berg, S. A.; Ravoo, B. J. Dynamic Reactions of Liposomes. *Soft Matter* **2014**, *10*, 60−65.
(20) Liang, J.; Huang, Y.; Zhang, L.; Wang, Y.; Ma, Y.; Guo, T.; Chen, Y. Molecular-Level Dispersion of Graphene into Poly(vinyl alcohol) and Effective Reinforcement of their Nanocomposites. *Adv. Funct. Mater.* **2009**, *19*, 2297−2302.
(21) Hummers, W. S.; Offeman, R. E. Preparation of Graphitic Oxide. *J. Am. Chem. Soc.* **1958**, *80*, 1339−1339.
(22) Xu, Y.; Zhao, L.; Bai, H.; Hong, W.; Li, C.; Shi, G. Chemically Converted Graphene Induced Molecular Flattening of 5,10,15,20-Tetrakis(1-methyl-4-pyridinio) porphyrin and Its Application for Optical Detection of Cadmium(II) Ions. *J. Am. Chem. Soc.* **2009**, *131*, 13490−13497.
(23) Chamberlain, M. M.; Bailar, J. C. The Infrared Spectra of Some Thicyanatocobalt Ammines. *J. Am. Chem. Soc.* **1959**, *81*, 6412−6415.
(24) Zhang, H. B.; Zheng, W. G.; Yan, Q.; Yang, Y.; Wang, J. W.; Lu, Z. H.; Ji, G. Y.; Yu, Z. Z. Electrically Conductive Polyethylene Terephthalate/graphene Nanocomposites Prepared by Melt Compounding. *Polymer* **2010**, *51*, 1191−1196.
(25) Dreyer, D. R.; Park, S.; Bielawski, C. W.; Ruoff, R. S. The Chemistry of Graphene Oxide. *Chem. Soc. Rev.* **2010**, *39*, 228−240.
(26) Ricciardi, R.; Mangiapia, G.; Lo Celso, F.; Paduano, L.; Triolo, R.; Auriemma, F.; De Rosa, C.; Laupretre, F. Structural Organization of Poly(vinyl alcohol) Hydrogels Obtained by Freezing and Thawing Techniques: A SANS Study. *Chem. Mater.* **2005**, *17*, 1183−1189.
(27) Ricciardi, R.; Auriemma, F.; De Rosa, C.; Laupretre, F. X-ray Diffraction Analysis of Poly(vinyl alcohol) Hydrogels, Obtained by Freezing and Thawing Techniques. *Macromolecules* **2004**, *37*, 1921−1927.
(28) Kou, L.; Gao, C. Bioinspired Design and Macroscopic Assembly of Poly(vinyl alcohol)-coated Graphene into Kilometers-long Fibers. *Nanoscale* **2013**, *5*, 4370−4378.
(29) Qusous, A.; Parker, E.; Geewan, C.; Kapasi, A.; Getting, S. J.; Hucklebridge, F.; Keshavarz, T.; Kerrigan, M. J. P. Novel Methods for the Quantification of Changes in Actin Organization in Chondrocytes using Fluorescent Imaging and Linear Profiling. *Microsc. Res. Technol.* **2012**, *75*, 991−999.
(30) Chen, G. Y.; Pang, D. W. P.; Hwang, S. M.; Tuan, H. Y.; Hu, Y. C. A Graphene-based Platform for Induced Pluripotent Stem Cells Culture and Differentiation. *Biomaterials* **2012**, *33*, 418−427.


DOI: 10.1021/acsami.5b00184
*ACS Appl. Mater. Interfaces* 2015, 7, 3003−3008